

Velocity model determination by the SMART method, Part 2: Application SP3.8

Jacques Jacobs, Delphine Sinoquet, Bertrand Duquet

► **To cite this version:**

Jacques Jacobs, Delphine Sinoquet, Bertrand Duquet. Velocity model determination by the SMART method, Part 2: Application SP3.8. SEG Annual meeting, Oct 1995, Houston, United States. hal-02284185

HAL Id: hal-02284185

<https://hal-ifp.archives-ouvertes.fr/hal-02284185>

Submitted on 11 Sep 2019

HAL is a multi-disciplinary open access archive for the deposit and dissemination of scientific research documents, whether they are published or not. The documents may come from teaching and research institutions in France or abroad, or from public or private research centers.

L'archive ouverte pluridisciplinaire **HAL**, est destinée au dépôt et à la diffusion de documents scientifiques de niveau recherche, publiés ou non, émanant des établissements d'enseignement et de recherche français ou étrangers, des laboratoires publics ou privés.

SUMMARY

The SMART (Sequential Migration Aided Reflection Tomography) method, as explained in the first part of this paper, starts after a first set of traveltimes in the unmigrated prestack data has been picked and the inventarization of useful a priori knowledge related to these traveltimes has been made. Thereto a preparative phase is needed.

First a global estimate of the subsurface structure is made. Hereto we use the standard stacking and poststack interpretation procedures which 'allow for getting insight in the degree of complexity of the subsurface. Next the traveltimes can be picked. When interpreting prestack data important qualitative structural information in difficult target zones (e.g. fault zones or salt structure flanks) can be obtained. Such an analysis guides the interpreter in selecting and picking the best traveltimes of primary events.

Once the preparation is finished the SMART method can be applied for a detailed determination of a structural and velocity model in a very consistent way. It is emphasized that velocity variations in complex structures can be determined accurately by prestack travelttime inversion techniques. This phase has an iterative character. In order to update the velocity model after the first iteration additional traveltimes are needed. Next additional traveltimes are obtained by interpretation of the cube of migrated data which can be easier than in the time domain due to the focussing and positioning effect of the migration process. By tracing rays in the same velocity model as was used for migration on the newly interpreted events, we will obtain additional traveltimes which will make the set of input data for the next iteration of tomography more complete. A new velocity model is calculated and the data are remigrated.

In this paper we will demonstrate the feasibility of this approach using a 2D real data set. We executed a number of iterations of the SMART method and ended up with a very satisfactory and reliable depth image of the complex structure.

THE DATA

We used for this application a 2D dataset covering a salt structure. It consists of 300 shotrecords at a regular interval of 40m. The acquisition was done in a split spread. The half spread length is 1920 meters with 48 geophones. The data were delivered with a standard preprocessing (filtering, zero-phase deconvolution and muting). Because of some clearly visible groundroll, we applied a second filter in order to remove most of this low frequency noise. A partial stack of the data is shown in Figure 1.

THE PREPARATIVE PHASE

Analysis of complexity

In order to get an idea of the degree of complexity of a subsurface, it is useful to construct several partial stacks with the same stacking velocity model. Because the stacking process is based on flattening of the hyperbola's in CMP's, through some NMO and DMO based correction, differences in between the partial stacks demonstrate the failure of the process. In areas with complex subsurface structures these hyperbola's aren't necessarily flat due to different raypaths left and right

of the midpoint. In this dataset this phenomenon can be observed in a series of CMP's covering the salt dome (See Figure 2).

Another way to get an idea of the complexity is to do a post stack depth migration by a layer stripping approach using the best partial stack. For these data the results are satisfactory for the sedimentary zones left and right of the dome, but are incorrect for the deep interfaces and the base of the salt. This is partially due to events that are lost during the stacking procedure. Other causes for this failure are: the uncertainty in picking the right interface that serves as the next velocity boundary and the difficult choice of the velocities which becomes more and more hazardous as the depth increases. The final result is unreliable and the resulting depth for the base of the salt depends largely on the choices made by the interpreter

Clearly these data cannot be handled by standard processing techniques. Left and right of the salt dome and below it the nature of the trace gathers is too complex. A prestack imaging method using a velocity model computed by tomography seems adequate for solving the aforementioned problems.

Data preparation for the SMART method

The next step after the analysis of the complexity is the data preparation for the SMART method. Its goal is to prepare an initial set of traveltimes to be used in the first iteration. We split this phase in a number of consecutive sub-phases:

- Creating a initial set of guides for the prestack interpretation.
- Picking traveltimes.
- Quality control of the traveltimes.
- Selection of representative traveltimes and calculation of the associated weights.

Creating a set of guides.

Guides are indicators for the interpreter suggesting where to look in the prestack unmigrated data for a certain event. They are also warnings for complicated situations as multiples, triplications and situations were no reliable indications for the nature of an event is available. The geologic guides are qualitative (e.g. presence of a fault) or quantitative (e.g. the depth of horizon A is 2500m). The geophysical guides are for example the presence of multiples or diffractions. They are derived from the unstacked or stacked data.

For this dataset the following data were used: a set of (partial) stacks, time- and depth-migrated stacks and the cube of preprocessed prestack data. It allowed us to determine the zones where picking traveltimes directly in the unmigrated data could lead to incorrect travelttime information for the tomography. These zones are indicated in Figure 1 (Za and Zb, a zone with triplications and a series of unexplained events.

Picking the first set of traveltimes

Using the guides the picking of the traveltimes can start. This is done in the cube of unmigrated data. There is no preference for picking in a specific trace gather. This depends of the available guide. When it is a geological one the common offset gathers are most suited. Using a geophysical one the interpretation is done in the shotgathers or the common midpoint gathers. Whatever direction is chosen, one has to end

up with one consistent surface describing the set of prestack traveltimes for one reflector.

Quality control of the traveltimes.

For those reflectors for which split spread data are available we analyzed to what extent the principle of reciprocity is fulfilled. The criterion of reciprocity can help the interpreter to find gross errors in his interpretation. An example is shown in Figure 3. There is a strong correlation visible between traveltimes along one specific offset. This is an indication that the offset has been picked incorrectly. The interpretation has been corrected and the strong offset-related errors were removed.

A second control consists of the calculation of the difference between an ideal hyperbola and the picked traveltimes. Given the traveltimes sorted per CMP, the 'stacking velocity' for each CMP can be calculated. It informs the interpreter about the regularity of his interpretation. We call this the CMP difference plot. Going from one geophone position to another the difference in traveltimes should be reasonable; that is to say within the limits of the standard interpretation error which is usually estimated to be 8 ms.

Selection of representative traveltimes and calculation of the associated weights.

Not all of the traveltimes picked are really needed for our implementation of reflection tomography. It is possible to give weights to each picked traveltime so that in less complex parts of the seismic data a selection of traveltimes is sufficient for obtaining the same result as if all traveltimes were used, of course at a significant lower computational cost. The selection of representative traveltimes is based on the analysis of the aforementioned CMP difference plots. They give a qualitative measure of the regularity of the velocity field above the reflector. For these data it was decided in the less complex parts to resample the set of traveltimes at every 500m for the line coordinate and every 80m for the receiver coordinate. In the complex zones these spacings were smaller.

The next step is to calculate the weights that have to be specified for the objective function used for reflection tomography. Our weights are a function of distance between the selected shot positions and receiver positions and the estimated residue associated to each set of traveltimes from one reflector. The latter one is obtained by taking the mean value for the difference between the set of picked traveltimes and the set of ideal CMP hyperbolas as calculated for the CMP difference plot.

The first set of traveltimes

The final set of traveltimes used for the first iteration of the SMART method was constituted as follows: For each reflector a list of selected traveltimes was established as function of the regularity of the CMP difference plot. For each set an estimation of the residue was made and the associated weights were calculated. At the end of this phase the traveltimes of 12 reflections were picked. The selected events are depicted in Figure 1. Those indicated with a dashed line were difficult to pick.

THE SMART ITERATIONS

After completion of the preparative phase, the phase in which the ultimate accuracy for both velocity and structural model is sought can be started. Our strategy is based on the SMART method. This interpretive prestack approach requires the following steps:

- a Processing of the traveltimes by reflection tomography
- 1 Depth migration of the seismic data or application of the PICLI method (See Part 1 of this paper) with the model obtained in the previous step
- 1 Interpretation of the prestack migrated data. Try to find important geological events which aren't flat in the coherency panels.
- a Computation of the traveltimes associated with the picked events in the migrated data by means of raytracing.
- a Adding these traveltimes to the already existing set of traveltimes
- 1 Repeat this sequence until a satisfactory depth image is obtained; hence the name of the method Sequential Migration Aided Reflection Tomography. In complex structures like this one a number of iterations is needed in order to find the minimum set of traveltimes that allows for an accurate determination of the velocity model.

We executed a number of iterations. Each iteration improved the velocity model as could be concluded from the increasing flatness of the coherency panels and the more and more geological image that was obtained after stacking the prestack depth migrated common offset gathers.

First iteration

For first iteration only the most reliable traveltimes as picked in the preparative phase were used. For this reason the traveltimes of the deep 'base of the salt' reflector were not included. The picking of these traveltimes in the unmigrated data was quite difficult and it was expected that after the first iteration of the SMART method they could be better determined in the cube of migrated common offset gathers. As a consequence the velocity model determined by tomography was only correct for the regions above the salt. However the effect of the migration on the deeper interfaces allowed us to pick in the cube the events associated with the base of the salt. After obtaining the associated traveltimes, it was possible to add to the set of earlier picked traveltimes, a great number of traveltimes associated with the base of the salt.

Second iteration

With these additional traveltimes - departing from the previous model - a new velocity model was calculated. The velocity model is depicted in Fig 4. The lines are those parts of the reflectors that are determined by the tomography. The data were migrated. The post migration stack is shown in Figure 5. For the upper part, as could be expected the result of migration didn't change much. However the base of the salt became now more visible and at the left side where a maximum of traveltimes could be furnished, a very good definition of the subsurface was found. The mean residues for most of the inverted reflectors are very low (2 msec to 10 msec). In regions where no or little traveltimes could be prepared the model and thus the result of migration is rather disappointing. However when comparing this result with the conventional stack, it can be easily concluded that even in this case, picking of the base of the salt as a continuous event is easier than in any time section.

The coherency panels are presented in Figure 6. The panel at 2000m indicates that the velocity model is quite correct. The event D is slightly dipping, probably because of the little number of traveltimes that are available at the left border of the dataset. The event G is flat. The strongly dipping events in between them are multiples. Deeper there are a number of more or less flat events, that correspond with the base of the salt. In the central part of the data, where no traveltimes were available, the model is highly undetermined and as a consequence the coherency

panel at 8000m doesn't show any flat event. Between 3000 and 4000m depth **some events** are visible. They correspond with the base of the salt. Clearly there will be no image of this part of the base of the salt in the stack. At the right side of the dome at 10000 m the panel shows some continuous but dipping events. In that zone too little traveltimes were available for correctly determining the velocity model. The event marked P is one of the reflectors of the sedimentary sequence right of the dome. Somewhere below the base of the salt should be visible. It can be probably found around 3800m.

Interesting are the residues associated to the interfaces J and G. The residues on G are very low, corresponding with the flat events in the coherency panels. However at the interface J close to the dome the residues are relatively high. Therefore the traveltimes were corrected for this interface. The event has been repicked in the depth domain and better traveltimes were obtained after raytracing. Apart from a number of corrections, new traveltimes were added.

Third iteration

After the addition of these traveltimes it was expected to arrive at a very good definition of velocity model. It turned out that again the residues for almost all inverted times were very low. The model is shown in Figure 7. After migration of the data the individual common offset gathers were of a much better quality than those as obtained in the second iteration. However the data due to the presence of groundroll are rather noisy. This migrated noise has the tendency to mask in the central part the weak reflectors of the base of the salt. Therefore we decided to apply instead of a migration the PICLI method on these data. The stack together with a number of coherency panels is shown in Figures 8 and 9. When comparing these results with those obtained in the second iteration, it is easy to observe the improvement of the imaging of the deeper part of the data. The salt base is correctly (flat and continuous) defined at the right side. This is especially due to the additional traveltimes associated with the sediments right of the dome. The PICLI method removed migration artefacts between 6000 and 9000m which made the continuation still more pronounced. At the left side where we added intermediate traveltimes associated with the unconformity the presence of a small fault in the basement can be observed.

In the coherency panel at 2000m there is now a clearly continuous event. Above the salt event there aren't so many changes, because we didn't change the traveltimes neither the a priori information. The most striking difference can be found in the coherency panel at 8000m. We improved the traveltime information of the upper sediments and we added traveltimes left and right of the dome. As a consequence great parts of the model between 6000 and 9000m are now better determined yielding a better migrated image. The panel at 10000m gives also a better image of the base of the salt. There are not so much improvements for the reflectors between 1200 and 2200m. This is probably related to extend of the corrections applied on the traveltimes in the second iteration.

The interpretability of the migrated data has become excellent, so that in a next iteration it will be possible to add still a few more traveltimes for those reflectors for which the coherency panels aren't completely flat.

CONCLUSIONS

Using a 2D dataset covering a really complex structure we have shown that standard processing cannot resolve the imaging problems related to complex wave propagation in such situations.

We have demonstrated the feasibility of the velocity determination method called SMART when applied on real data.

ACKNOWLEDGMENTS

The data for this article were kindly provided by Shell. This research was rried out as part of the Prestack Structural Interpretation Consortium Project (PSI). The authors hereby acknowledge the support provided by e sponsors of this project.

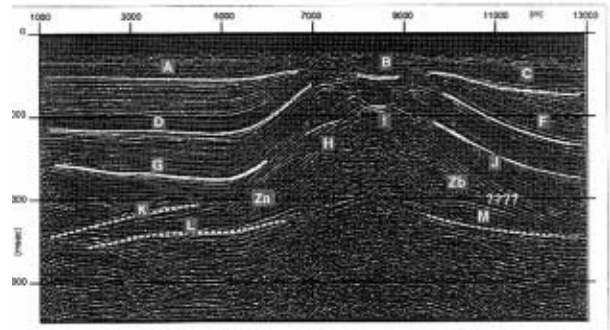


Figure 1 Unmigrated partial stack. The events for which traveltimes are picked are indicated by solid or dashed lines according to the reliability of the picking.

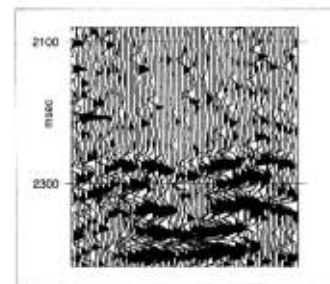


Figure 2 A part of a CMP gather at 6000m. Note the non-hyperbolic character of the reflector at 2300 msec.

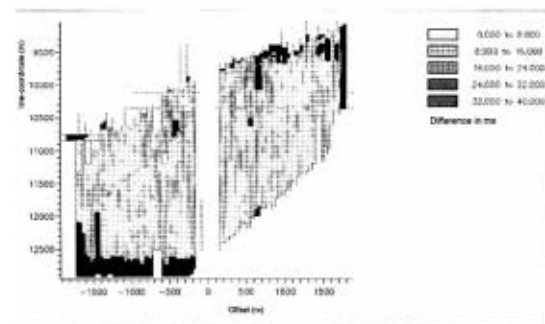


Figure 3 Reciprocity analysis of the event G. Note the strong correlation along the offset axis.

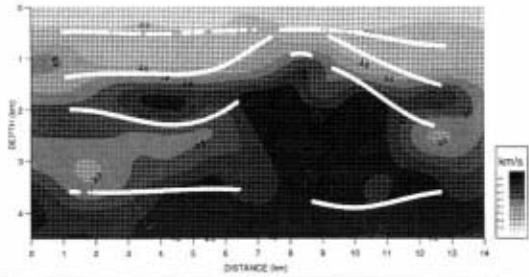


Figure 4 The model calculated by tomography in the second iteration

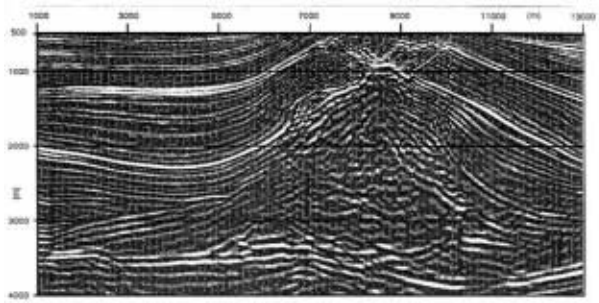


Figure 5 The post migration stack of the second iteration

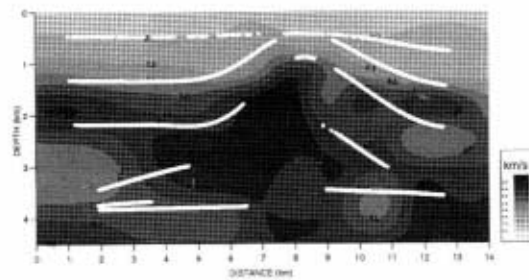


Figure 7 The model calculated by tomography in the third iteration

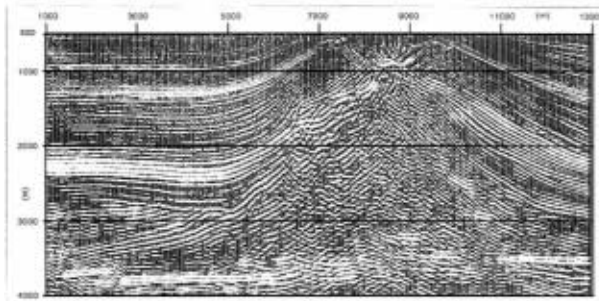


Figure 8 The post migration stack of the third iteration

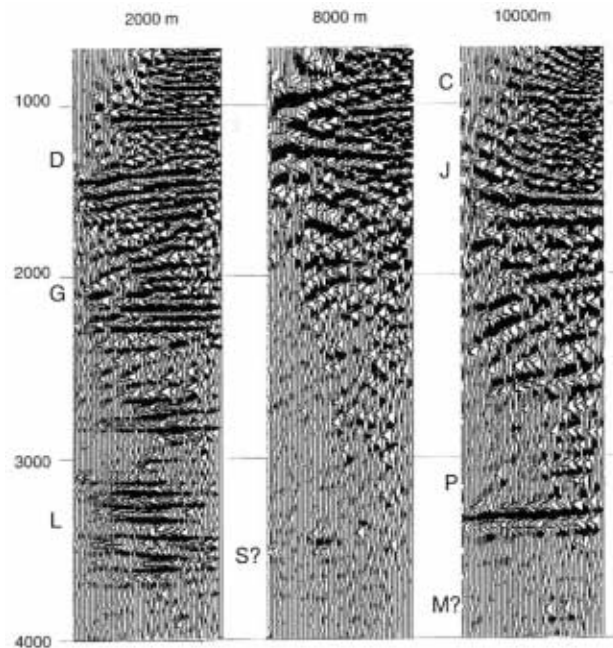


Figure 6 Three representative coherency panels (second iteration)

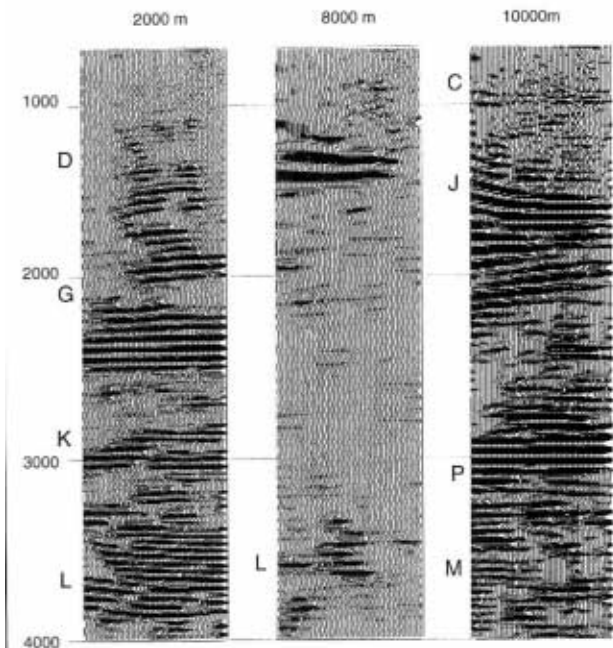


Figure 9 Three representative coherency panels (third iteration)